American Journal of Engineering Research (AJER) ***2021***
American Journal of Engineering Research (AJER)
e-ISSN: 2320-0847 p-ISSN : 2320-0936
Volume-10, Issue-05, pp: 275-291
www.ajer.org
Research Paper Open Access

Fault detection energetic approach through Directed Behavioral Hypergraph Formalism

Dhaou GARAI [1], Rafika EL HARABI [2], Faouzi BACHA [1]
[1]*LISI Laboratory, INSAT / Carthage University, Tunisia,*
[2] *Macs Laboratory, University of Gabes, Tunisia*
Corresponding Author: Dhaou GARAI. LISI Laboratory, INSAT / Carthage University, Tunisia,

ABSTRACT : *In the present paper, an alternative causal graph based fault detection scheme is designed. The quantitative reasoning is based on the Hamiltonian bond graph HBG, because the graphical model use combining the bond graph BG and the port Hamiltonian PH formalism for characterizing of energy interactions between submodels, is here used for to design the energetic fault signature matrix EFSM is generated from the energetic residuals ERs for the fault detection of the physical systems. The qualitative reasoning, we capture the qualitative effects of faults on the measurements using the directed behavioral hypergraph (DBH) derived from (HBG) model. And then, we compared and discussed the qualitative and quantitative approaches to demonstrate their diagnostic, detection and isolability of defects over the system.*
KEYWORDS : *Fault diagnosis, Hamiltonian bond graph, energetic residuals, directed behavioral hypergraph.*

Date of Submission: 12-05-2021 Date of acceptance: 25-05-2021

I. INTRODUCTION

The last few decades witnessed an increasing demand for efficient dynamic systems that operate at their maximum performance. However, the rate of component failures increases with the physical systems complexity. These malfunctions are called faults, and appropriate actions have to be calculated using fault control strategies. In order to avoid these problems, some fault detection and isolation algorithms have played an important role in several fault detection and isolation (FDI) approaches [1]. A trustworthy model allowing an appropriate representation of the behavior of dynamic systems is necessary to provide appropriate fault diagnostic models for physical processes. Well-established approaches to fault diagnosis are based on an analytically associated model or graphically associated representations [2]. Actually, the mathematical representation cannot allow energy interactions between a number of physical elements [3].

The bond graph BG approach is based on the observation of energetic exchanges among the system components and can be applied to dynamic systems and to any physical domain. [3]. Once the fault is detected, the Bond Graph topology is then applied in order to identify the actual fault source [4].

The Port-Hamiltonian PH formalism is of great importance regarding the dynamic systems fault detection and isolation modeling of owing to the many advantages it may offer, which explains to the reason for preserving a particular structure [5].

Among the important aspects of the port-Hamiltonian formalism is that it allows the display of the relation between energy storage , energy dissipation and the interconnection structure. This strategy represents the physics of the dynamic system [6]. Therefore, the Port-Hamiltonian (PH) formalism is very suitable to formalize the Bond Graph BG model of a dynamic system [7]. In this paper, a new approach was proposed through the combination between two formalisms (PH and BG) to design a fault detection algorithm [8].

The quantitative graphical approach is one the approaches for fault detection and isolation (FDI) community using the Hamiltonian Bond Graph model HBG [9] and based on the Energetic Residuals (ERs) generation. Basically, ERs is a redundant equation that verifies the link between the physical system model in normal operation, and the real process measurements. These can be checked directly from the Hamiltonian bond graph model developed in [10]. Moreover, the energetic residuals ERs represent the energy conservation equations of the interacting physical systems, and they are obtained by use of the HBG model causal structure. The Energetic Fault Signature Matrix (EFSM) is generated from the energetic residuals ERs, in order to conclude about fault isolability [19].

Hypergraphs are considered as a generalization of graphs allowing the representation of the causal relationships between the variables and the dynamic system parameters [8]. These techniques are involved in many areas of sciences [11] and they are useful even in engineering applications [12]. Recently, the hypergraph methodology has been considered as a good candidate in a System of Systems organization design [14]. The authors discussed in more details the usefulness of this approach in the monitoring of defaults [13]. This model can be used for establishing control and diagnosis approaches allowing the detection of any abnormality affecting a dynamic system [15]. The qualitative reasoning relies on the principle of consistency [12] . In this research study, we used the Hamiltonian Bond Graph HBG in an integral causality model to improve the fault detection and isolation procedure. We captured the qualitative effects of faults on the measurements using the Directed Behavioral Hypergraph (DBH) derived automatically from the HBG model. The DBH captures the causal relationships between the variables and the physical system parameters. The defined rules consist in converting each HBG element into a weighted directed hyperedge from input to output variables. Constitutive relations of nodes must comply with the physics conservation laws. Then, the causality involved in the system elements has an influence on the orientation of the hyperedge, and also generates the qualitative fault signature matrix QFSM.

This work provides three major contributions. First, the design of novel Hamiltonian Bond Graph HBG approach that takes into account the energetic aspect, the suggested scheme is the combination of two formalisms, to design the energetic fault signature matrix EFSM which is generated from the energetic residuals ERs. Second, we developed a Directed Behavioral Hypergraph DBH model from the Hamiltonian bond graph HBG, and proposed some Junction and elements transformations. Third, we conceived an FDI algorithm based on the structural, behavioral and causal properties of the directed behavioral hypergraph DBH associated to dynamic systems. Subsequently, the DBH model description obtained from the Hamiltonian Bond Graph modeling was applied for the qualitative analysis of the IDE tasks. Compared to the Hamiltonian bond graph HBG model based residual signals, the developed method is able to minimize the number of the qualitative redundancy relationships QRRs taking into account the qualitative state of known variables. It aims to improve the performances and the monitoring time through this fault generation scheme. The case study shows the effectiveness of the developed approach, without any numerical calculation. Finally, we presented a systematic framework for comparison after presenting the quantitative fault signature method and the qualitative fault signature method.

This paper is organized as follows. Section II introduced the graphical tools for modeling. Section III displayed a DC motor system case study. Finally, Section IV was dedicated to draw our conclusions and suggest some future perspectives.

II. GRAPHICAL APPROACHES FOR MODELING

In this section, the proposed methodology is based on the combined analysis of quantitative and qualitative reasoning as detailed in Figure 1. We focused on two graphical modeling tools: First, the quantitative reasoning based on the combination between two formalisms PH and BG [16] was introduced. Second, we proposed a Qualitative reasoning fault signature method, derived from the Directed Behavioral Hypergraph model DBH [14]. This model is generated in a systematic way relying on the architecture of the dynamic system. However, the Directed Behavioral Hypergraph Model DBH was extracted from the HBG model.

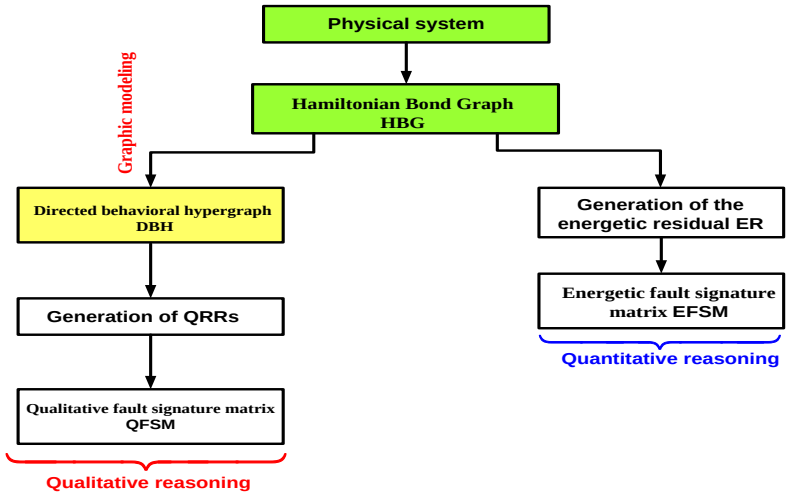

Fig.1. Combined quantitative and qualitative reasoning.

II.1. Quantitative graphical approach

1. Bond Graph Formalism BG

The bond graph tool can process several equations representing the behavior of the physical system and allow an explicit display of the interactions and interconnections between the different components of the system[3]. The interchanged energy between two variables A and B, is depicted through a bond (half-arrow) and reflects the physical structure. The causal stroke shows the direction of the pair of flow $f\ (t)$ and effort $e\ (t)$ variables [19]. The single or coupled energy BG modeling includes accumulative (storage C-element or inertia I-element), dissipative (R-element), as seen in Figure2.

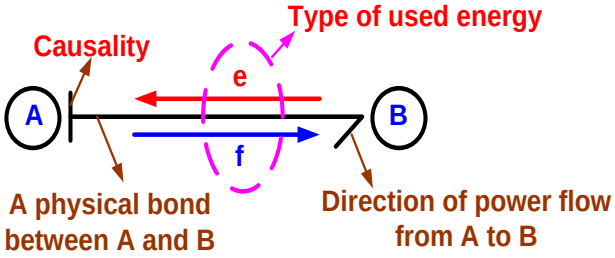

Fig 2. Bond Graph representation

2. Port-Hamiltonian formalism PH

As a unified language for representing dynamic systems, the Port-Hamiltonian formalism is based on the power aspect and the energy dissipation and accumulation phenomena. Thus, the power and energy variables can be clearly shown via associated frameworks using the Dirac structure and the Bond Graph models. So, combining the Port-Hamiltonian systems that are well-founded on the Dirac structures and the Bond graph tool can afford a novel way to study and embed structural and behavioral concepts [17]. It is worth noting that the Port-Hamiltonian formalism is considered as an adequate way to formalize the bond graph description [18]. In the classic form, the Port-Hamiltonian system can be described as:

$$\begin{cases} \dot{x} = (J(x) - R(x))\nabla H(x) + G(x)u \\ Y = G(x)^T \nabla H(x) \end{cases} \quad (1)$$

where x indicates the state variables (the energy accumulations). **J(x)** is a skew symmetric matrix $J(x) = -J(x)^T$. **R(x)** is a symmetric positive semi definite matrix $R(x) = R(x)^T \geq 0$, representing the energy dissipation. Denoting the Dirac structure of the system. **H** is a function of the state and is considered as the system energy, while the power-conjugated variables are, respectively, the input **u** and the output **y** [19].

3. Combining BG and PH formalisms

From a geometric point of view, the Dirac structure is essential in the description of (PH) systems, and has a strong link with Bond Graphs (BG), mainly that junctions 0 and 1 are first order examples of a Dirac structure [9]. We can think of the Hamiltonian Bond Graph HBG model graph as a graphical representation based on the transfer of energy in a system taking into account the Hamilton energy. The main elements of a Port-Hamiltonian (PH) are the notion of junction structures, indicated in Figure 2 through, **1** junction, **0** junction, TF , or GY . These structures are linked to properties of the energy preservation, that is to say, the junction joins the port variables in such a way that the total energy associated with all the port variables is 0, as seen in Figure3 [9].

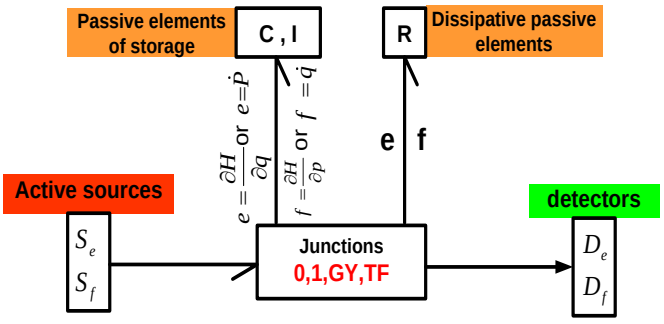

Fig 3. Generalized Hamiltonian Bond Graph elements.

3. Diagnosis based on HBG

The energetic behavior of the physical system are expressed through the following relation:

$$\dot{H} = \left(\nabla H\ (x)^T\ \dot{x}\right) = \underbrace{\nabla H\ (x)^T\ J(x)}_{P_C\ =\ 0} \nabla H\ (x) - \underbrace{\nabla H\ (x)^T\ R\ (x)}_{Q\ \geq\ 0} \nabla H\ (x) + Y^T U_{P_{ext}}$$

Each physical system, even if it is several energy domains, can be represented by a HBG model. These approaches are based on the comparison between the behavior of the system and the reference behavior taking [19]. The energy residuals ERs are derived from the Hamiltonian bond graph HBG model through the procedures of unknown variables elimination. Indeed, the residual signals describe the dynamic or static constraint energetic relations. Each time the energy residuals ERs are designed, the fault detection step checks whether they are very satisfied or not. We can consider E as the nominal energy of a system, which can be equal to:

$$E = \int u^T\ y \tag{2}$$

E_s is the stored energy of the Hamiltonian system in a fault-free case, which can be equal to:

$$E_s = \int \frac{\partial H}{\partial x}^T \dot{x} \tag{3}$$

or

$$E_s = \int \dot{x}^T \frac{\partial H}{\partial x} \tag{4}$$

There is an energy-storing function E_s for the dissipative Hamiltonian system such that the inequality holds as the following relation shows:

$$E_s \leq \int u^T\ y \tag{5}$$

There exists a positive energy dissipation function E_d :

$$E_d = \int e_R^T\ f_R \tag{6}$$

the nominal energy E of the Hamiltonian system, can be equal to:

$$E = E_s + E_d = \int u^T y \tag{7}$$

Based on the above described energy balance, the energy residual ER function of the Hamiltonian Bond Graph at each junction is represented as follows:

$$ER\ :\ R = E_s + E_d - \int u^T y \tag{8}$$

The energy residual ER is obtained from the comparison of the energy quantity $\int u^T y$ determined in a nominal case and the two energy quantities E_s and E_d based on the junctions of the Hamiltonian Bond Graph modeling. A fault is detected if the energy residual ER of the junctions is greater than 0.

II.2. Qualitative graphical approach

1. Definition1: (Directed Behavioral Hypergraph DBH).

A Directed Behavioral Hypergraph (DBH) is a Directed Hypergraph used as the model to perform behavioral adaptations. Let $H = (V, \varepsilon)$ be a directed hypergraph obtained from the HBG–DBH analog (or

transformation). The DBH can be systematically build from the HBG model using a relevant algorithm according to the following steps:

1. Construct the HBG model.

2. Identify all HBG elements and transform them into weighted directed hyperedges from input to output variables and the orientation of each hyper-edge is simply and performed through the respect of the same HBG causality stroke corresponding to elements. As well, obtaining the constitutive relationships of nodes must take into account energy-conserving physical principles (energy, power, back-effects) and particular physical interpretations.

3. Put together different elements and nodes to establish the BDH representation of the system.

Remark 1.

Note that the weights assigned to the hyper-edges $w(\varepsilon)$ is defined as a numerical value for two-port elements, while as a matrix with multiple values for multi-port elements. so the following notation is used:

- ✓ the set of input flows I_f is equal to the set of output flows O_f .
- ✓ the set of input efforts I_e is equal to the set of output efforts O_e .

2. Bond Graph- Directed Behavioral Hypergraph transformations

To get graphical model systems by developing a Directed Behavioral Hypergraph **DBH** model from the **HBG**, we proposed the elements transformations given in Table 1, and the Junction elements transformations given in Table (2).

Table 1: Elements transformations HBG-DBH

Element	Bond Graph	Causal equation	Directed Behavioral Hypergraph	hyperedge weight
Dissipative passive elements **R**	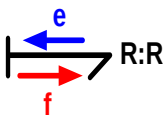	$e = R \cdot f$	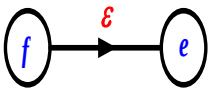	$W(\varepsilon) = R$
	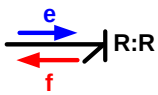	$f = \frac{1}{R} . e$	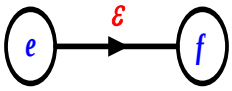	$W(\varepsilon) = \frac{1}{R}$
passive elements of storage **I**	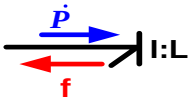	$f = \frac{1}{I} . P$	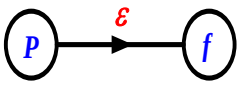	$W(\varepsilon) = \frac{1}{I}$
	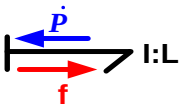	$P = I . f$	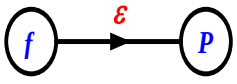	$W(\varepsilon) = I$
passive elements of storage **C**	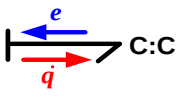	$e = \frac{1}{C} . q$	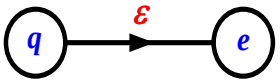	$W(\varepsilon) = \frac{1}{C}$
	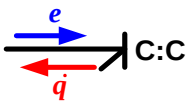	$q = C . e$	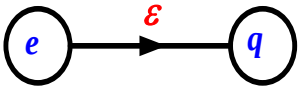	$W(\varepsilon) = C$

Table 2: Junctions transformations HBG-DBH

junctions	HBG	Causal equation	DBH	hyperedge weight
0-junction	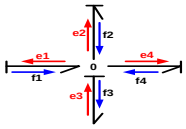	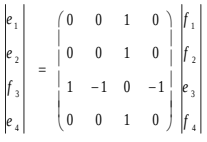	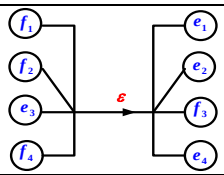	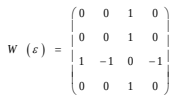
1-junction	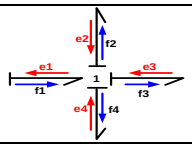	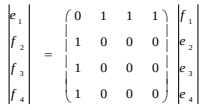	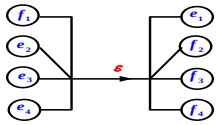	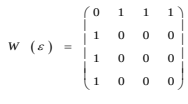
TF-junction	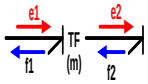	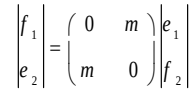	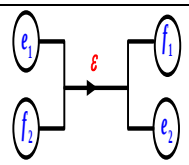	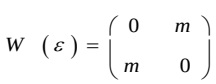
	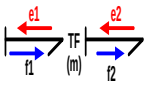	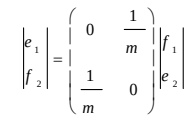	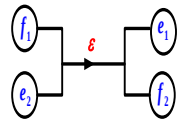	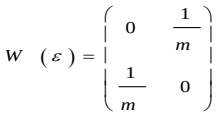
GY-junction	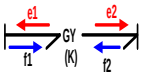	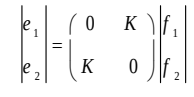	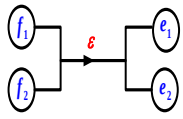	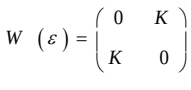
	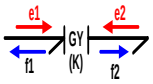	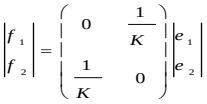	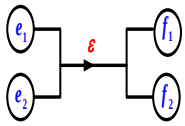	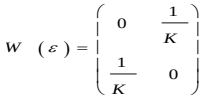

3. Directed Behavioral Hypergraph based for qualitative FDI design

Our purpose was to generate redundancy relationships for surveillance using directed behavioral hypergraph DBH model. The algorithm which we give will look for the shortest paths connecting an unknown variable to known variables on the DBH model.

- **Algorithms for QRRs generation**

The proposed QRR generation algorithm functioning can be summarized as follows:

1. Collecting the unknown variables on the model: $K = \{unknown\ variables\}$
2. Choosing an element υ_i in the set K.
3. Finding all the output hyperedges ε_{io} of υ_i .
4. Finding the shortest path connecting υ_i across ε_{io} to all measurable variables.
5. The $V_o(\varepsilon_{io})$ corresponds to the set of measurable variables in the shortest path found.
6. Finding the set of input hyperedges ε_{iI} of υ_i .
7. Finding the shortest path way connecting υ_i across ε_{iI} to all measurable variables.
8. The $V_I(\varepsilon_{iI})$ corresponds to the set of measurable variables in the shortest path found.
9. finding the qualitative redundancy relationship through: $QRR_i = \{-V_I(\varepsilon_{iI}), V_o(\varepsilon_{io})\}$
10. Taking the following element from the set K.
11. If the QRR of this element is different from the other QRRs, then save it; otherwise, consider another element from K.
12. Repeating the step 10 until all the unknown variables are considered and all the independent signatures are obtained.

- **Qualitative fault signature matrix QFSM**

The structure of the residual forms a matrix S_{ij} that expresses discrepancy in which component i (sensors, actuators and physical devices) can change the value of residual j .

Given the QRR set of QRRs, the signature of a fault F_i is given by the vector $SF_i = [S_{i1}, S_{i2} \ldots\ldots\ldots S_{in}]$

whose S_{ij} is defined by the following application: $S : F \times QRR \rightarrow \{0, -, +\}$

$$(F_i, QRR_j) \longrightarrow S_{ij} = \begin{cases} + \ If \ \ F_i \ \ is \ involved \ \ with \ a \ sign + \ \ in \ QRR \\ - \ If \ \ F_i \ \ is \ involved \ \ with \ a \ sign - \ \ in \ QRR \\ 0 \quad otherwise \end{cases}$$

III. CASE STUDY: DC MOTOR

The considered process is a DC motor, was presented to demonstrate the effectiveness of the proposed energy-based fault detection approach, namely the Hamiltonian Bond Graph HBG modeling, as shown in Figure 4.

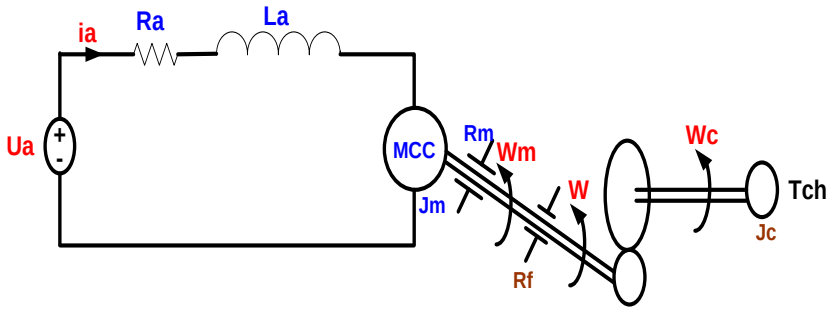

Fig 4. Synoptic of the DC Motor

The parameter values related to the DC Motor are indicated in table 3.

Table 3: Parameters of the DC motor

R_a	Armature resistance	8 Ω
L_a	Armature inductance	$0.129\ H$
k	Constant torque	0.7745
J_m	shaft inertia	$0.02\ kg.m^2$
R_m	Viscous friction	$0.0218\ Nm/s$
m	Reducer coefficient	0.25
J_c	inertia of load	$0.0037\ kg.m^2$
R_f	coupling friction	$100\ Nm/s$

III.1. Quantitative approach based on HBG model

Figure 5 displays the Hamiltonian bond graph in integral causality of the DC motor:

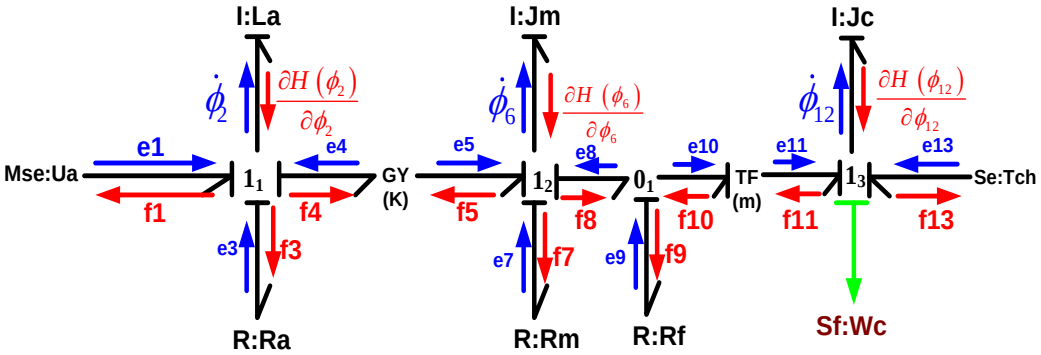

Fig.5. HBG Model in an integral causality.

From the trained Hamiltonian bond graph HBG model, we can deduce a state representation equivalent to this graph and is expressed as follows:

$$\begin{pmatrix} \dot{\phi}_2 \\ \dot{\phi}_6 \\ \dot{\phi}_{12} \end{pmatrix} = \begin{pmatrix} -R_a & -K & 0 \\ K & -(R_m + R_f) & mR_f \\ 0 & mR_f & -m^2 R_f \end{pmatrix} \begin{pmatrix} \frac{\phi_2}{L_a} \\ \frac{\phi_6}{J_m} \\ \frac{\phi_{12}}{J_c} \end{pmatrix} + \begin{pmatrix} 1 & 0 \\ 0 & 0 \\ 0 & -1 \end{pmatrix} \begin{pmatrix} u \\ T_{ch} \end{pmatrix} \tag{9}$$

The classic formulation of the Hamiltonian system with ports Equation 9 can be rewritten as follows:

$$\begin{cases} \begin{pmatrix} \dot{\phi}_2 \\ \dot{\phi}_6 \\ \dot{\phi}_{12} \end{pmatrix} = \left[\begin{pmatrix} 0 & -K & 0 \\ K & 0 & 0 \\ 0 & 0 & 0 \end{pmatrix} - \begin{pmatrix} R_a & 0 & 0 \\ 0 & R_m + R_f & -mR_f \\ 0 & mR_f & m^2 R_f \end{pmatrix} \right] \cdot \begin{pmatrix} \frac{\phi_2}{L_a} \\ \frac{\phi_6}{J_m} \\ \frac{\phi_{12}}{J_c} \end{pmatrix} + \begin{pmatrix} 1 & 0 \\ 0 & 0 \\ 0 & -1 \end{pmatrix} \cdot \begin{pmatrix} U \\ T_{ch} \end{pmatrix} \\ y = \begin{pmatrix} 1 & 0 \\ 0 & 0 \\ 0 & -1 \end{pmatrix} \cdot \begin{pmatrix} \frac{\phi_2}{L_a} \\ \frac{\phi_6}{J_m} \\ \frac{\phi_{12}}{J_c} \end{pmatrix} \end{cases} \tag{10}$$

With $J(x) = \begin{pmatrix} 0 & -K & 0 \\ K & 0 & 0 \\ 0 & 0 & 0 \end{pmatrix}$, $R(x) = \begin{pmatrix} R_a & 0 & 0 \\ 0 & R_m + R_f & -mR_f \\ 0 & mR_f & m^2 R_f \end{pmatrix}$ and $G(x) = \begin{pmatrix} 1 & 0 \\ 0 & 0 \\ 0 & -1 \end{pmatrix}$

The derivative hamiltonian bond graph DHBG model is presented in figure 6.

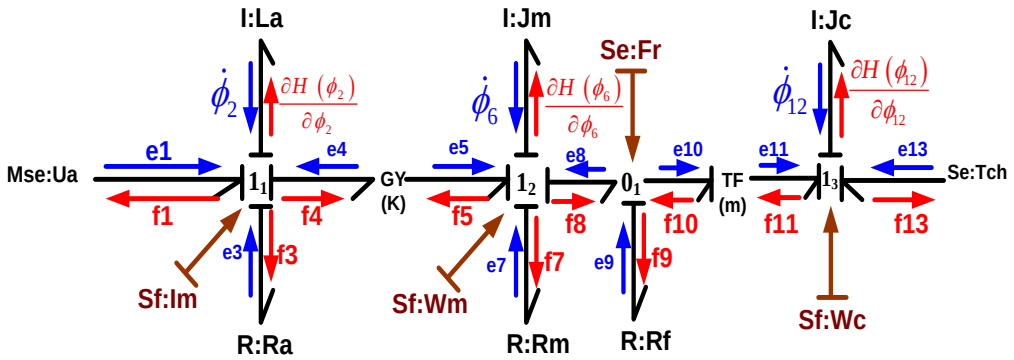

Fig.6. HBG Model in derivative causality.

The energy residual ER is obtained from the junction 1_1 of the HBG formalism which can be rewritten as:

$$ER_1 : \int \phi_2^{'T} \frac{\partial H(\phi_2)}{\partial \phi_2} + \int \left(R_a \frac{\partial H(\phi_2)}{\partial \phi_2} \right)^T \frac{\partial H(\phi_2)}{\partial \phi_2} + \int \left(K \frac{\partial H(\phi_6)}{\partial \phi_6} \right)^T \frac{\partial H(\phi_2)}{\partial \phi_2} - \int u_a^T \frac{\partial H(\phi_2)}{\partial \phi_2} = 0 \quad (11)$$

Or $\frac{\partial H(\phi_2)}{\partial \phi_2} = I_m$, $\frac{\partial H(\phi_6)}{\partial \phi_6} = W_m$ and $\frac{\partial H(\phi_{12})}{\partial \phi_{12}} = W_c$

The energetic residuals on the HBG model is based on the elimination of unknown variables (Equation 11), using the structural properties of junction 1_1, the obtained energetic residual is:

$$ER_1 : \int \left(L_a \frac{d}{dt} . I_m \right)^T I_m + \int (R_a . I_m)^T I_m + \int (K . W_m)^T I_m - \int u_a^T . I_m = 0 \quad (12)$$

The energy residual ER is obtained from the junction 1_2 of the HBG formalism which can be rewritten as:

$$ER_2 : \int \dot{\phi}_6^T \frac{\partial H(\phi_6)}{\partial \phi_6} + \int \left(R_m \frac{\partial H(\phi_6)}{\partial \phi_6} \right)^T \frac{\partial H(\phi_6)}{\partial \phi_6} + \int F_r^T \frac{\partial H(\phi_6)}{\partial \phi_6} - \int \left(K \frac{\partial H(\phi_2)}{\partial \phi_2} \right)^T \frac{\partial H(\phi_6)}{\partial \phi_6} = 0 \quad (13)$$

The determination of energetic residuals is based on the elimination of unknown variables. Form equation 13, the obtained energetic residual of junctions 1_2 is:

$$ER_2 : \int \left(J_m \frac{d}{dt} . W_m \right)^T W_m + \int (R_m . W_m)^T W_m + \int F_r^T . W_m - \int (K . I_m)^T W_m = 0 \quad (14)$$

The energy residual ER is obtained from the junction 0_1 of the HBG model which can be rewritten as:

$$ER_3 : \int F_r^T \left(\frac{\partial H(\phi_6)}{\partial \phi_6} - m \frac{\partial H(\phi_{12})}{\partial \phi_{12}} \right) + \int F_r^T m \frac{\partial H(\phi_{12})}{\partial \phi_{12}} - \int F_r^T \frac{\partial H(\phi_6)}{\partial \phi_6} = 0 \quad (15)$$

The determination of the energetic residuals is based on the elimination of unknown variables seen in Equation 17; the obtained energetic residual of junctions 0_1 is then:

$$ER_3 : \int F_r^T (W_m - m W_c) + \int F_r^T m W_c - \int F_r^T W_m = 0 \quad (16)$$

The energy residual ER is obtained from the junction 1_3 of the HBG formalism which can be rewritten as:

$$ER_4 : \int \dot{\phi}_{12}^T \frac{\partial H(\phi_{12})}{\partial \phi_{12}} - \int (m . F_r)^T \frac{\partial H(\phi_{12})}{\partial \phi_{12}} - \int T_{ch}^T \frac{\partial H(\phi_{12})}{\partial \phi_{12}} = 0 \quad (17)$$

The determination of energetic residuals is based on the elimination of unknown variables seen in Equation 17, the obtained energetic residual of junctions 1_3 is then:

$$ER_4 : \int \left(J_c \frac{d}{dt} . W_c \right)^T W_c - \int (m . F_r)^T W_c - \int T_{ch}^T W_c = 0 \quad (18)$$

In quantitative reasoning, the energetic fault signature matrix EFSM is given by Table 4. We have observed that all sensor faults are detected and isolated.

Table 4 : Energetic Fault Signature Matrix EFSM

	ER_1	ER_2	ER_3	ER_4	D	I
I_m	1	1	0	0	1	1
W_m	1	1	1	0	1	1
F_r	0	1	1	1	1	1
W_c	0	0	1	1	1	1

Simulation results

For our simulation, we used the 20-sim software (version 4.7), the simulation diagram is given in figure 7.

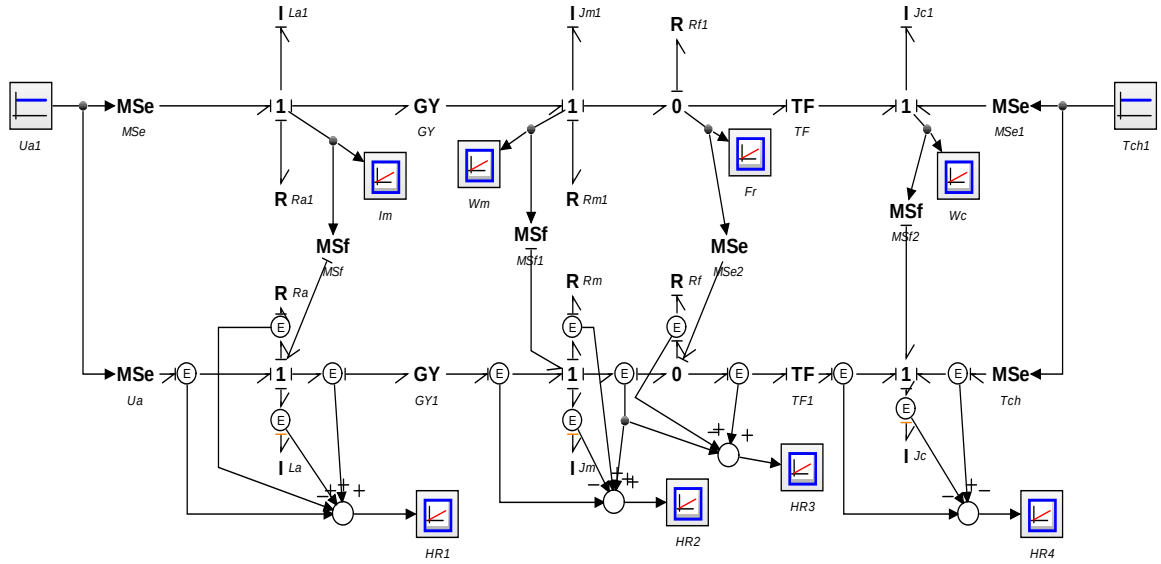

Fig.7. HBG modeling Scheme

The parameters of the DC motor are shown in Table 3. The control input signal is $u_a = 47.3V$, and the load torque T_{ch} is modulated by a signal.

We can clearly observe the paths of the state variable I_a and the state variable W_m and W_c (see figures 8 and 9) .

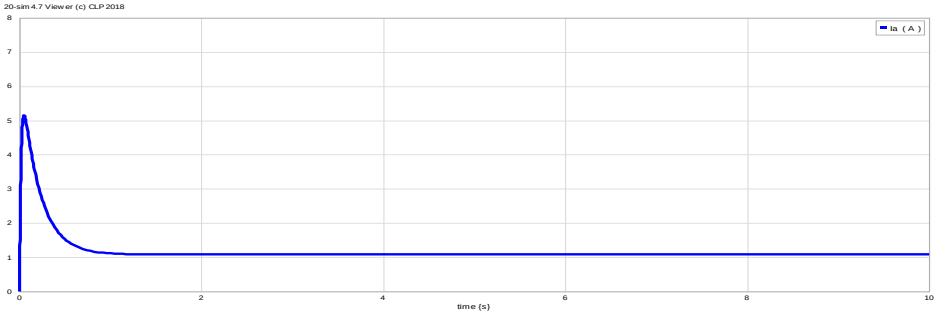

Fig.8. The armature current I_a .

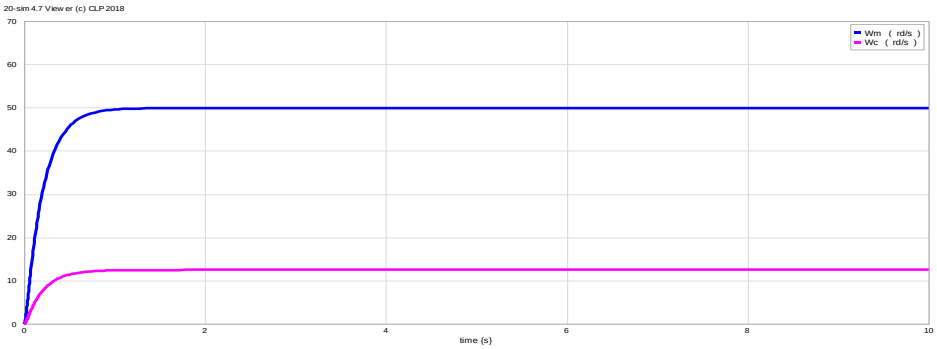

Fig.8. The velocity Wm and Wc

It is clear that in a fault –free case, the energy residual ER_1 , ER_2 , ER_3 and ER_4 signals are equal to zero, (see figure 9).

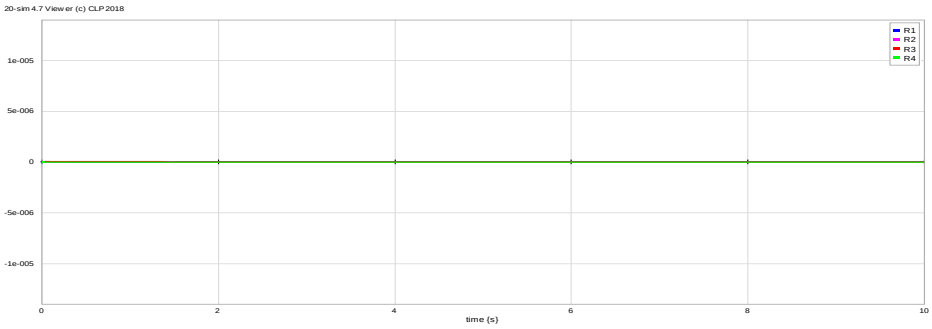

Fig.9. The energy residual Ers

To test the effectiveness of the designed method, two types of faults (actuator and sensor) were taken into account in the simulation.

An actuator fault with additive form occurred between the instants 4s and 5s. Figures 10 and 11 illustrate the simulation result. Therefore, the outputs were discarded from their nominal values.

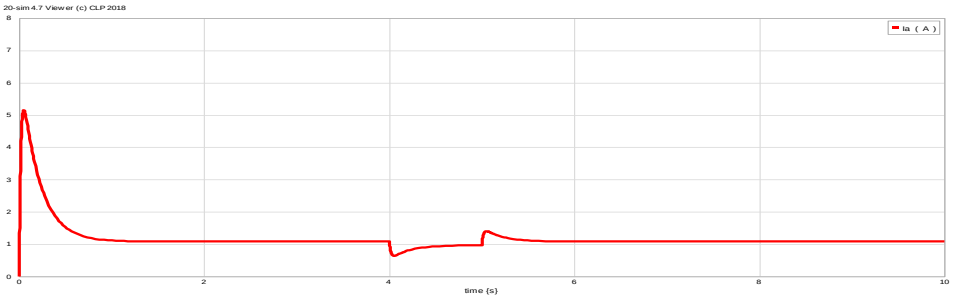

Fig.10. The armature current I_a

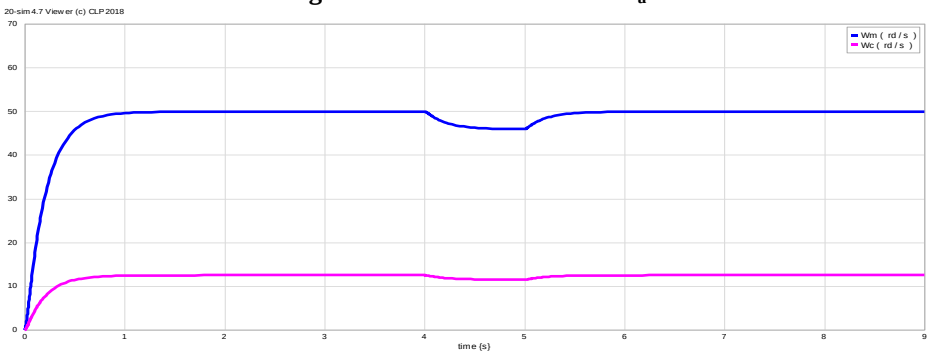

Fig.11. Velocity state Response in a faulty situation.

The actuator fault was detected by the residual energy ER1 when it appeared. It was equal to the amount of energy injected by the fault into the system at the time interval $[3s\ ,10s]$. However, the residual energy signals ER2, ER3 and ER4 are equal to zero (see figure 12).

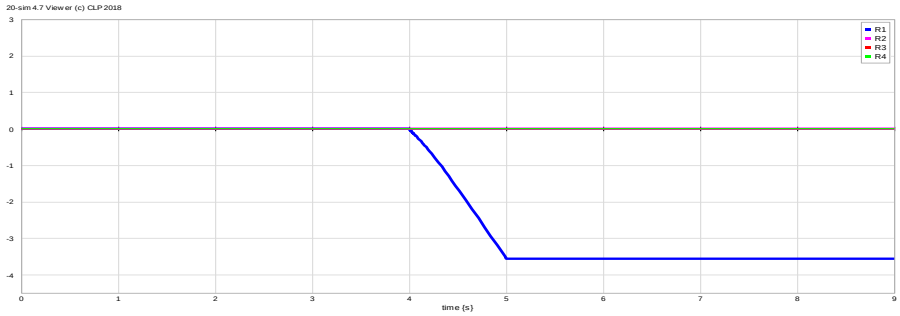

Fig.12. The energy residual case of the actuator fault.

We supposed the occurrence of a sensor fault I_m during the time interval $[4s, 5s]$. In this case, the presence of the sensor fault affected only the intensity response I_a, which justifies the allure of the energetic residual (see fig. 13).

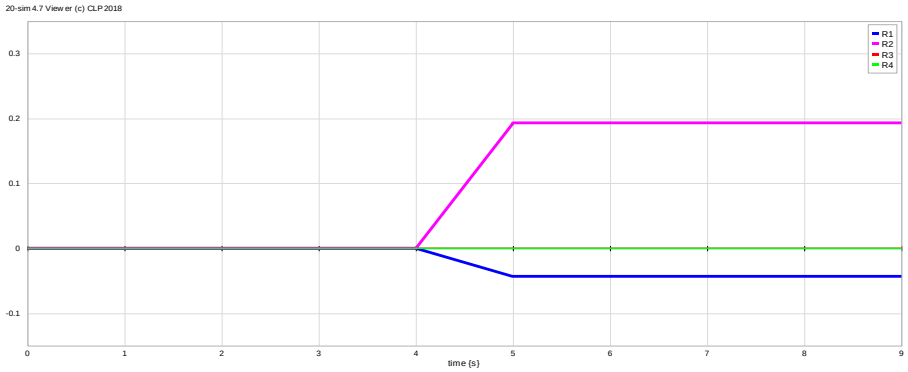

Fig.13. The energy residual case of the sensor fault.

The energy residual ER_1 and ER_2 is equal to the energy amount injected by the sensor fault I_m into the system at the time interval $[4s, 10s]$.

The primary objective of the fault detection task has been achieved since the residual energy generators are used to distinguish between faulty and fault-free situations.

III.2. Qualitative approach based on DBH model

In qualitative reasoning, the goal is to generate redundancy relationships for fault monitoring using the directed behavioral hypergraph DBH model.

The Directed Behavioral Hypergraph model $H_d = (V_d, \varepsilon_d)$ consists of twenty one vertices

$$V_d = \left\{ \begin{array}{c} U_a, T_{ch}, I_m, W_m, F_r, W_c, \dot{\phi}_2, \dot{\phi}_6, \dot{\phi}_{12}, e_3, \\ e_4, e_5, e_7, e_8, e_{11}, f_9, f_{10}, f_{11}, \phi_2, \phi_6, \phi_{12} \end{array} \right\}$$

and fifteen hyperedges $\varepsilon_d = \left\{ \begin{array}{c} \varepsilon_1, \varepsilon_2, \varepsilon_3, \varepsilon_4, \varepsilon_5, \varepsilon_6, \varepsilon_7, \varepsilon_8, \\ \varepsilon_9, \varepsilon_{10}, \varepsilon_{11}, \varepsilon_{12}, \varepsilon_{13}, \varepsilon_{14}, \varepsilon_{15} \end{array} \right\}$

where $\varepsilon_1 = (\{I_m, U_a, e_3, e_4\}, \{\dot{\phi}_2, I_m, I_m, I_m\})$, $\varepsilon_2 = (\{\phi_2\}, \{I_m\})$, $\varepsilon_3 = (\{\dot{\phi}_2\}, \{\phi_2\})$, $\varepsilon_4 = (\{I_m\}, \{e_3\})$

$\varepsilon_5 = (\{I_m, W_m\}, \{e_4, e_5\})$, $\varepsilon_6 = (\{W_m, e_5, e_7, e_8\}, \{\dot{\phi}_6, W_m, W_m, W_m\})$, $\varepsilon_7 = (\{\phi_6\}, \{W_m\})$ $\varepsilon_8 = (\{\dot{\phi}_6\}, \{\phi_6\})$

$\varepsilon_9 = (\{W_m\}, \{e_7\})$, $\varepsilon_{10} = (\{W_m, F_r, f_{10}\}, \{F_r, f_9, F_r\})$, $\varepsilon_{11} = (\{f_9\}, \{F_r\})$ $\varepsilon_{12} = (\{F_r, W_c\}, \{f_{10}, e_{11}\})$,

$\varepsilon_{13} = (\{W_c, e_{11}, T_{ch}\}, \{\dot{\phi}_{12}, W_c, W_c\})$ $\varepsilon_{14} = (\{\phi_{12}\}, \{W_c\})$ and $\varepsilon_{15} = (\{\dot{\phi}_{12}\}, \{\phi_{12}\})$

The DBH model deduced from different junctions are is given in table 5.

Table 5: DBH model from different junctions

Junctions	Structural laws	DBH
Junction $\mathbf{1}_1$	$\begin{vmatrix} \dot{\phi}_2 \\ I_m \\ I_m \\ I_m \end{vmatrix} = \begin{pmatrix} 0 & 1 & -1 & -1 \\ 1 & 0 & 0 & 0 \\ 1 & 0 & 0 & 0 \\ 1 & 0 & 0 & 0 \end{pmatrix} \begin{vmatrix} \frac{\partial H(\phi_2)}{\partial \phi_2} \\ U_a \\ e_3 \\ e_4 \end{vmatrix}$ $f_1 = \frac{\partial H(\phi_2)}{\partial \phi_2} = f_3 = I_m$	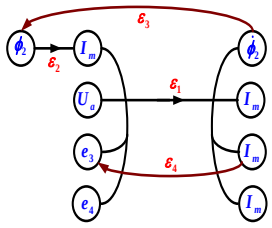
Junction GY	$\begin{vmatrix} e_4 \\ e_5 \end{vmatrix} = \begin{pmatrix} 0 & K \\ K & 0 \end{pmatrix} \begin{vmatrix} I_m \\ W_m \end{vmatrix}$ $f_4 = I_m \quad , f_5 = W_m$	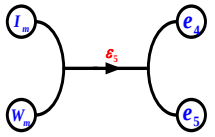
Junction $\mathbf{1}_2$	$\begin{vmatrix} \dot{\phi}_6 \\ W_m \\ W_m \\ W_m \end{vmatrix} = \begin{pmatrix} 0 & 1 & -1 & -1 \\ 1 & 0 & 0 & 0 \\ 1 & 0 & 0 & 0 \\ 1 & 0 & 0 & 0 \end{pmatrix} \begin{vmatrix} \frac{\partial H(\phi_6)}{\partial \phi_6} \\ e_5 \\ e_7 \\ e_8 \end{vmatrix}$ $f_5 = \frac{\partial H(\phi_6)}{\partial \phi_6} = f_7 = f_8 = W_m$	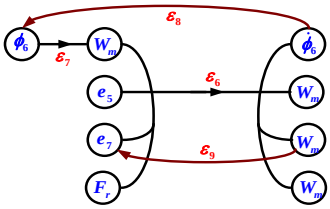
Junction $\mathbf{0}_1$	$\begin{vmatrix} F_r \\ f_9 \\ F_r \end{vmatrix} = \begin{pmatrix} 0 & 1 & 0 \\ 1 & 0 & -m \\ 0 & 1 & 0 \end{pmatrix} \begin{vmatrix} W_m \\ F_r \\ f_{10} \end{vmatrix}$ $e_8 = e_9 = e_{10} = F_r$	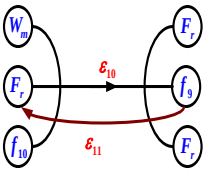
Junction TF	$\begin{vmatrix} F_r \\ W_c \end{vmatrix} = \begin{pmatrix} 0 & m \\ m & 0 \end{pmatrix} \begin{vmatrix} f_{10} \\ e_{11} \end{vmatrix}$ $f_{11} = W_c \ , \ e_{10} = F_r$	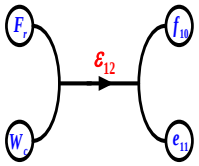

Junction 1_3	$\begin{vmatrix} \dot{\phi}_{12} \\ W_c \\ W_c \end{vmatrix} = \begin{pmatrix} 0 & 1 & -1 \\ 1 & 0 & 0 \\ 1 & 0 & 0 \end{pmatrix} \begin{vmatrix} \frac{\partial H(\phi_{12})}{\partial \phi_{12}} \\ e_{11} \\ T_{ch} \end{vmatrix}$ $f_{11} = \frac{\partial H(\phi_{12})}{\partial \phi_{12}} = f_{13} = W_c$	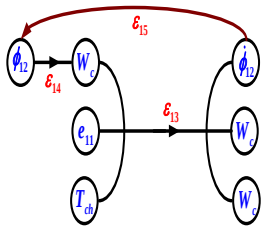

The Directed Behavioral Hypergraph model DBH of the DC motor Figure (14) was deduced from the Hamiltonian Bond Graph model, where an integral causality is shown in Figure 5 and given by.

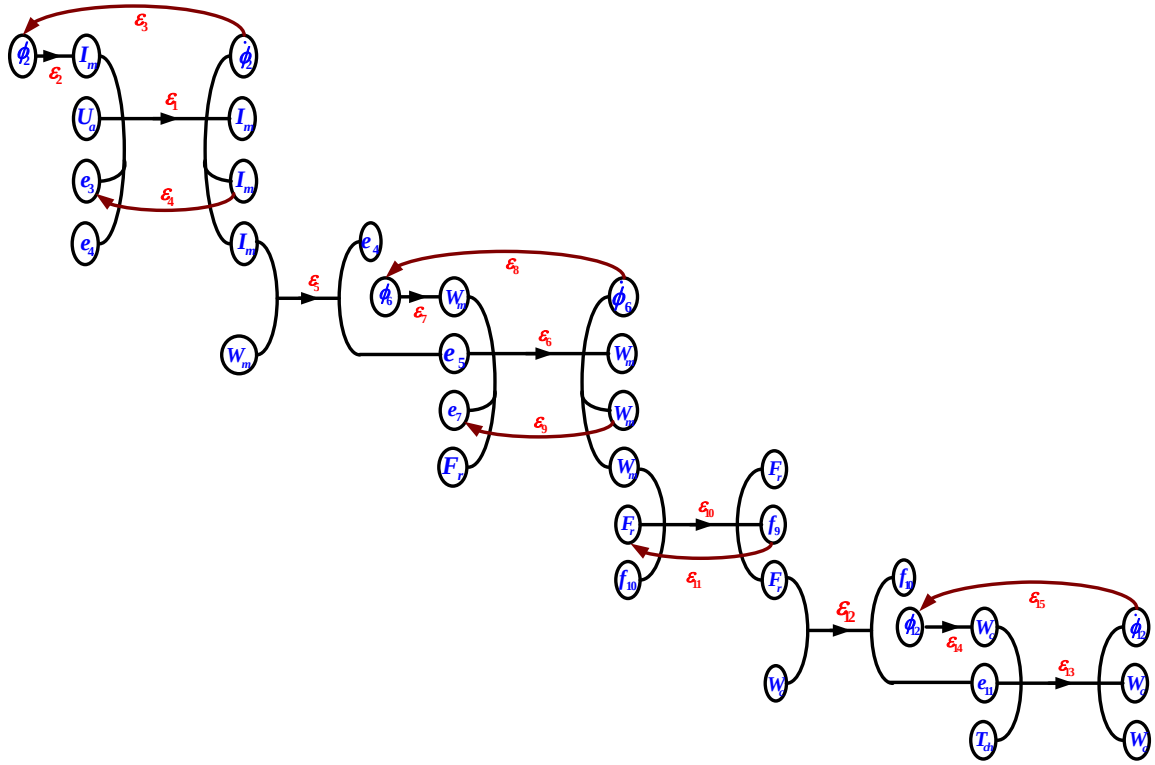

Fig.14. Directed Behavioral Hypergraph DBH model.

From the Directed Behavioral Hypergraph model DBH (see figure 14), we have three variables that are not measurable that are $\dot{\phi}_2$, $\dot{\phi}_6$ and $\dot{\phi}_{12}$ (the set of unknown variables $K = \{\dot{\phi}_2, \dot{\phi}_6, \dot{\phi}_{12}\}$).

- The two hyperedges ε_1 and ε_3 are adjacent via the variable $\dot{\phi}_2$. ($\varepsilon_1 \cap \varepsilon_3 = \{\dot{\phi}_2\}$), where both hyperedges contain measurable variables (see figure 15).

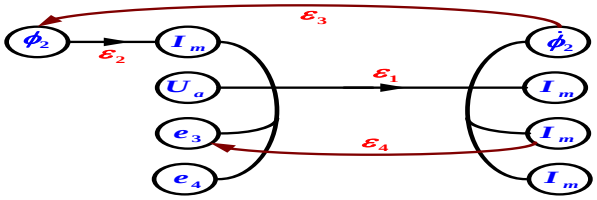

Fig.15. The adjacent hyperedges via variable $\dot{\phi}_2$

The hyperedge ε_3 is the output hyperedge of $\dot{\phi}_2$: $\dot{\phi}_2 \rightarrow \varepsilon_3 \rightarrow \phi_2$, $(\phi_2 = L_a I_m) \Rightarrow V_O(\varepsilon_3) = \{I_m\}$

The hyperedge ε_1 is the input hyperedge of $\dot{\phi}_2$: $\dot{\phi}_2 \leftarrow \varepsilon_1 \leftarrow \{U_a, e_3, e_4\}, e_3 = R_a I_m, e_4 = K W_m \Rightarrow V_I(\varepsilon_1) = \{U_a, I_m, W_m\}$

Hence, the first relationship redundancy is deduced:

$$QRR_1 = \{-U_a, -W_m, I_m\} \tag{19}$$

- The two hyperedges ε_6 and ε_8 are adjacent via the variable $\dot{\phi}_6$. ($\varepsilon_6 \cap \varepsilon_8 = \{\dot{\phi}_6\}$), where both hyperedges contain measurable variables (see figure 16).

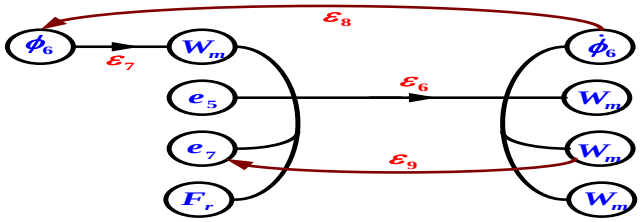

Fig.16. The adjacent hyperedges via variable $\dot{\phi}_6$.

The hyperedge ε_8 is the output hyperedge of $\dot{\phi}_6$: $\dot{\phi}_6 \rightarrow \varepsilon_8 \rightarrow \phi_6, (\phi_6 = J_m W_m) \Rightarrow V_O(\varepsilon_8) = \{W_m\}$

The hyperedge ε_6 is the input hyperedge of $\dot{\phi}_6$: $\dot{\phi}_6 \leftarrow \varepsilon_6 \leftarrow \{e_5, e_7, F_r\}, e_5 = K I_m, e_7 = R_m W_m \Rightarrow V_I(\varepsilon_6) = \{F_r, I_m, W_m\}$

Hence, the second relationship redundancy is deduced:

$$QRR_2 = \{-F_r, -I_m, W_m\} \tag{20}$$

- The two hyperedges ε_{13} and ε_{15} are adjacent via the variable $\dot{\phi}_{12}$. ($\varepsilon_{13} \cap \varepsilon_{15} = \{\dot{\phi}_{12}\}$), where both hyperedges contain measurable variables (see figure 17).

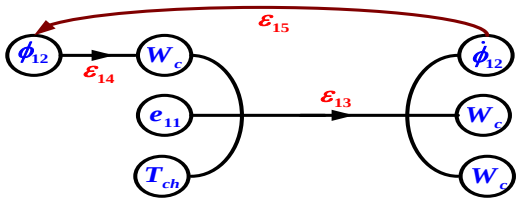

Fig.17. The adjacent hyperedges via variable $\dot{\phi}_{12}$

The hyperedge ε_{15} is the output hyperedge of $\dot{\phi}_{12}$: $\dot{\phi}_{12} \rightarrow \varepsilon_{15} \rightarrow \phi_{12}, (\phi_{12} = J_c W_c) \Rightarrow V_O(\varepsilon_{15}) = \{W_c\}$

The hyperedge ε_{13} is the input hyperedge of $\dot{\phi}_{12}$: $\dot{\phi}_{12} \leftarrow \varepsilon_{13} \leftarrow \{e_{11}, T_{ch}\}, e_{11} = m F_r \Rightarrow V_I(\varepsilon_{13}) = \{F_r, T_{ch}\}$

Hence, the third relationship redundancy is deduced:

$$QRR_3 = \{-F_r, W_c\} \tag{21}$$

The qualitative fault signature matrix QFSM is given by Table 6. We have observed that all sensor faults are detected and isolated.

Table 6 : Qualitative fault signature matrix QFSM

	QRR_1	QRR_2	QRR_3	D	I
I_m	+	-	0	1	1
W_m	-	+	0	1	1
F_r	0	-	-	1	1
W_c	0	0	+	1	1

The associated variable with each component was found to be present in at least one residue. So, all the faults of the system are theoretically detectable (D = 1). In addition, the components' signatures are unique, which means that the faults of these components are isolable (I = 1).

IV. Conclusion

In this paper, a primary description of a fault detectability and fault isolability analysis method has been based on Hamiltonian Bond Graph HBG. The advantage of the proposed methodology lies in the combined analysis of quantitative and qualitative reasoning and is mainly suitable for model-based fault monitoring, in the domain of multiport systems to understand the electromechanical system performance based on a combination of mechanical and electrical dynamics. For the quantitative reasoning, a set of the energetic residuals HRs can be derived systematically from the Hamiltonian Bond Graph HBG in an integral causality model. As shown in Table 4, the resulting energetic fault signature matrix EFSM derived from the HBG show the theoretical activation values of the energetic residuals ERs corresponding to the possible faults. The ERs approach has two advantages. First, the energy residues ERs can be derived automatically from the Hamiltonian Bond Graph Model in an Integral causality. Second, the actuator and sensor faults can be detected and isolated.

In the qualitative approach, using the Directed Behavioral Hypergraph DBH derived from the Hamiltonian Bond Graph HBG, we captured the qualitative effects of faults on the measurements to define the qualitative fault signature matrix QFSM which can be used to carry out a fault diagnosis. As displayed in Table 6, this approach enables detecting a fault from all the elements of the DC motor and obtaining good results for the isolation task for all the different faults that may affect the system.

As a future perspective, we will extend this analysis and comparison to nonlinear systems for the qualitative approach to cover parametric faults.

REFERENCES

[1]. BLANKE, Mogens, KINNAERT, Michel, LUNZE, Jan, et al. Diagnosis and fault-tolerant control. Berlin : springer, 2006.

[2]. BOUAMAMA, B. Ould, MEDJAHER, K., BAYART, M., et al. Fault detection and isolation of smart actuators using bond graphs and external models. Control engineering practice, 2005, vol. 13, no 2, p. 159-175.

[3]. DJEZIRI, Mohand Arab, BOUAMAMA, B. Ould, et MERZOUKI, Rochdi. Modelling and robust FDI of steam generator using uncertain bond graph model. Journal of process control, 2009, vol. 19, no 1, p. 149-162.

[4]. EL HARABI, Rafika, SMAILI, Rahma, et ABDELKRIM, Mohamed Naceur. Fault diagnosis algorithms by combining structural graphs and PCA approaches for chemical processes. In : Chaos Modeling and Control Systems Design. Springer, Cham, 2015. p. 393-416.

[5]. JELTSEMA, Dimitri et DORIA-CEREZO, Arnau. Port-Hamiltonian formulation of systems with memory. Proceedings of the IEEE, 2011, vol. 100, no 6, p. 1928-1937.

[6]. ORTEGA, Romeo, VAN DER SCHAFT, Arjan, MASCHKE, Bernhard, et al. Interconnection and damping assignment passivity-based control of port-controlled Hamiltonian systems. Automatica, 2002, vol. 38, no 4, p. 585-596.

[7]. VAN DER SCHAFT, Arjan et JELTSEMA, Dimitri. Port-Hamiltonian systems theory: An introductory overview. Foundations and Trends in Systems and Control, 2014, vol. 1, no 2-3, p. 173-378.

[8]. AJEMNI, Henda, EL HARABI, Rafika, et ABDELKRIM, Mohamed Naceur. Directed Hypergraph model-based FDI of chemical reaction.

[9]. ATITALLAH, Manel, EL HARABI, Rafika, et ABDELKRIM, Mohamed Naceur. A comparative study of energetic model-based fault detection using HBG and COG formalisms. International Transactions on Electrical Energy Systems, 2017, vol. 27, no 9, p. e2363.

[10]. ATITALLAH, Manel, EL HARABI, Rafika, et ABDELKRIM, Mohamed Naceur. Fault detection and estimation based on full order unknown input Hamiltonian observers. In : 2015 IEEE 12th International Multi-Conference on Systems, Signals & Devices (SSD15). IEEE, 2015. p. 1-7.

[11]. AJEMNI, Henda, EL HARRABI, Rafika, et ABDELKRIM, Mohamed Naceur. Modeling of chemical reaction kinetics using Hypergraph tools. In : 2014 International Conference on Electrical Sciences and Technologies in Maghreb (CISTEM). IEEE, 2014. p. 1-6.

[12]. AJEMNI, H., EL HARABI, R., et ABDELKRIM, M. N. Directed Hypergraph-based Models for the Fault Monitoring of Chemical Reaction Kinetics. International Journal of Computer Applications, 2017, vol. 166, no 12.

[13]. KHALIL, Wissam, MERZOUKI, Rochdi, OULD-BOUAMAMA, Belkacem, et al. Hypergraph models for system of systems supervision design. IEEE Transactions on Systems, Man, and Cybernetics-Part A: Systems and Humans, 2012, vol. 42, no 4, p. 1005-1012.

[14]. ABDESSELAM, Ibtissam, HAFFAF, Hafid, et OULD-BOUAMAMA, Belkacem. Bond-graphs and hyper-graphs in system of systems modelling. International Journal of System of Systems Engineering, 2016, vol. 7, no 4, p. 313-338.
[15]. ABDESSELAM, Ibtissam et HAFFAF, Hafid. Hypergraph reconfigurability analysis. IERI Procedia, 2014, vol. 6, p. 22-32.
[16]. HÉLIE, Thomas, FALAIZE, Antoine, et LOPES, Nicolas. Systèmes Hamiltoniens à Ports avec approche par composants pour la simulation à passivité garantie de problèmes conservatifs et dissipatifs.
[17]. FALAIZE, Antoine. Modélisation, simulation, génération de code et correction de systèmes multi-physiques audios: Approche par réseau de composants et formulation Hamiltonienne À Ports. 2016. Thèse de doctorat.
[18]. HÉLIE, Thomas, FALAIZE, Antoine, et LOPES, Nicolas. Systèmes Hamiltoniens à Ports avec approche par composants pour la simulation à passivité garantie de problèmes conservatifs et dissipatifs.
[19]. GARAI, Dhaou, EL HARABI, Rafika, et BACHA, Faouzi. Hamiltonian Bond Graph formalism for generating energetic redundant relations. In : 2020 17th International Multi-Conference on Systems, Signals & Devices (SSD). IEEE, 2020. p. 1063-1068.

Dhaou GARAI, et. al. "Fault detection energetic approach through Directed Behavioral Hypergraph Formalism."*American Journal of Engineering Research (AJER)*, vol. 10(5), 2021, pp. 275-291.